A&A 402, 571–586 (2003)
DOI: 10.1051/0004-6361:20030268

Astronomy & Astrophysics

An X-ray study of the open clusters NGC 2451 A and B⋆,⋆⋆

M. Hünsch[1], C. Weidner[1], and J. H. M. M. Schmitt[2]

[1] Institut für Theoretische Physik und Astrophysik, Universität Kiel, Olshausenstraße 40, 24118 Kiel, Germany
[2] Hamburger Sternwarte, Universität Hamburg, Gojenbergsweg 112, 21029 Hamburg, Germany

Received 8 November 2002 / Accepted 15 January 2003

Abstract. We have conducted a detailed study of the object NGC 2451, which actually consists of two different open clusters A and B along the same line of sight at 206 pc and 370 pc distance, respectively. Although belonging to the nearest clusters, they have not been much investigated until present due to strong contamination by field stars. ROSAT X-ray observations and optical *UBVR* photometry are used to identify cluster members by means of X-ray emission and colour-magnitude diagrams. The identified stars concentrate nicely around the expected main sequences in the colour-magnitude diagram at the distances derived from astrometric investigations. Altogether, 39 stars are identified as member candidates of the nearer cluster A, 49 stars as member candidates of the more distant cluster B, and 22 faint stars are probably members of either of the two clusters, but due to large errors it is not clear to which one they belong. Further 40 stars identified with X-ray sources are probably non-members. For the first time, the range of known probable cluster members of NGC 2451 A and B has been extended downwards the main sequence to stars of spectral class M. Isochrone fitting yields an age of 50 to 80 Myrs for NGC 2451 A and ≈50 Myrs for NGC 2451 B, consistent with the X-ray luminosity distribution functions, which are comparable to other clusters in the same age range. Except from the occurence of four flares, the stars of both clusters do not show strong long-term X-ray variability exceeding a factor 5 over a time span of 1 to 3 years.

Key words. stars: activity – stars: coronae – Hertzsprung-Russell (HR) and C-M diagrams – open clusters and associations: individual: NGC 2451 – X-rays: stars

1. Introduction

During the last decade, much progress has been achieved in the study of the age-, mass- and metallicity-dependence of various stellar properties like activity, rotation, and lithium abundances from the observation of stellar clusters. Ideally, one would like to cover a large range of ages and metallicities to achieve a good sampling of these parameters and to prove whether a particular cluster can be regarded as representative of its age.

Concerning the evolution of stellar activity in the context of angular momentum loss on the main sequence, the main results are: i) a general decrease of rotational velocities and stellar activity with age, ii) for slow and moderately fast rotating stars, a good correlation between rotation or Rossby number (i.e., ratio of rotation period to convective turnover time) and X-ray luminosity, iii) increasing rotational spindown time scales with decreasing mass, iv) the existence of a saturation level in normalized X-ray emission ($\log L_x/L_{bol} \approx -3$) achieved above a threshold rotational velocity (or below a threshold Rossby number), which occurs at progressively earlier stars the younger the cluster is, v) a strong scatter (∼1 dex) in X-ray luminosities for stars in a given cluster (i.e., at the same age) and given spectral type, consistent with a similar spread in rotational rates that may have its origin in the individual history and details of the star formation processes (decoupling between circumstellar disk and star) within a given cluster.

However, a number of unsolved problems remain. For example, it is still not clear whether the age-activity relation is unique, and in particular, whether a cluster of a given age can be regarded as a representative for similar clusters in terms of activity. Various studies of similarly-old clusters (Hyades, Coma Berenices, Praesepe, IC 4756, NGC 6633) revealed marked differences in the mean activity level, which cannot be easily explained (cf. Randich & Schmitt 1995a; Randich et al. 1996a; Randich et al. 1998; Harmer et al. 2001; Barrado y Navascués & Stauffer 1998). There is also some evidence among younger clusters (NGC 6475 vs. Pleiades) violating the well-ordered activity sequence with age (cf. Randich 1997).

An additional problem arises from the large scatter of X-ray luminosities observed in the Pleiades and Hyades even for stars of similar rotation rates, which cannot be fully explained by measurement errors or unknown inclination angles

Send offprint requests to: M. Hünsch,
e-mail: huensch@astrophysik.uni-kiel.de

⋆ Based on observations performed by the ROSAT X-ray observatory and the European Southern Observatory.

⋆⋆ Tables 3–6 are only available in electronic form at http://www.edpsciences.org

(Micela et al. 1996; Stern et al. 1995) or short and long-term X-ray variability (Gagné et al. 1995; Stern et al. 1995; Schmitt et al. 1993).

A further issue not yet settled is the dependence of stellar activity on metallicity. In principle, one would expect stars of lower metallicity to have shallower convection zones, thus shorter convective turnover time scales and at the same rotation rate higher Rossby numbers than similar stars of solar metallicity. Hence, such stars should have either reduced X-ray emission or they do not follow the quite uniform Rossby number – normalized X-ray emission relation observed for various clusters. In NGC 2516, which originally was thought to be of lower than solar metallicity, Jeffries et al. (1997) and Micela et al. (2000) indeed find the G-type dwarfs to have lower X-ray luminosities than their counterparts in the Pleiades. However, recent spectroscopic observations (Terndrup et al. 2002) revealed that NGC 2516 is probably of Pleiades-like metallicity. We further note that X-ray observations of the metal-rich ([Fe/H] = +0.23) cluster Blanco 1 (Micela et al. 1999) do not suggest a significant role of metallicity in determining coronal properties.

From the observational point of view, a main problem is the sensitivity limit of the available X-ray observations if one wants to achieve sufficient sensitivity to detect solar-like X-ray emission. Additional problems arise from the lack of comprehensive membership studies for the majority of clusters, being a tedious effort based on colour-magnitude diagrams (CMDs) and proper motions.

Whereas a large amount of photometric studies exist for most known clusters, proper motion studies have been performed only for the nearer clusters and often only for the brighter stars. In this respect, the method of identifying cluster members by means of their X-ray emission turned out to be a powerful tool in the cases of several young clusters such as IC 2602, NGC 6475 (M 7), and NGC 2516 (Randich et al. 1995b; Prosser et al. 1995; Jeffries et al. 1997). However, one always has to keep in mind that this method introduces a bias towards X-ray bright objects, and that the derived XLDF may be affected.

In this paper, we present X-ray observations and optical photometry of the cluster NGC 2451, which actually consists of two different clusters along the same line of sight. Surprisingly, the clusters have hitherto been very little studied although NGC 2451 A belongs to the 10 nearest clusters. The clusters were originally believed to be of special interest due to their suspected low metallicity. However, a recent spectroscopic study by us (Hünsch et al. 2003) revealed that both clusters are very likely of solar metallicity. A further issue of interest are the three ROSAT pointings lying 1 and 3 years apart, thus allowing a study of X-ray variability in the clusters.

Details on the nature of the clusters and a summary of previous work is given in Sect. 2. ROSAT X-ray observations are reported in Sect. 3 while Sect. 4 comprises our own optical *UBVR* photometry. The problem of identifying cluster members is addressed in Sect. 5, and Sect. 6 reports the various properties of the clusters as derived by our study. Section 7 yields a comparison between NGC 2451 and similar clusters, followed by our conclusions in Sect. 8.

2. The nature of NGC 2451 – a historical review

NGC 2451 (= Collinder 161) was probably first noticed by G. B. Hodierna (1597–1660), who marked it as a nebulous patch in his star chart. The cluster was later on observed by John Herschel during his South African expedition (1834–1838) and found its way into J. L. E. Dreyer's New General Catalogue.

The first detailed study of the cluster was performed by Williams (1966, 1967a, 1967b) who obtained *UBV* photometric data of 213 stars within a 1 square-degree region around the bright star c Pup (=HD 63032). Williams derived an age of NGC 2451 of 2.3×10^7 yrs and a distance of 330 pc but noticed a large scatter of two magnitudes around the main sequence. At the same time, Feinstein (1966) found from his *UBV* photometry of 22 stars a distance of 260 pc and a considerably larger age of $\sim10^8$ yrs. Both authors quote little reddening of the order of $E(B-V)\approx0.05$.

Eggen (1983) concluded from the large spread of distance moduli derived from his own intermediate band and Hβ photometry that NGC 2451 is just a chance alignment of bright stars and, hence, that a cluster does not exist. On the other hand, Lyngå & Wramdemark (1984) argued on the basis of Eggen's own data that there is a concentration of stars and a well-defined main sequence if restricted to the brighter (i.e., B- and A-type) stars. This was subsequently confirmed by Eggen (1986) himself. Lyngå and Wramdemark also derived metal abundances from *uvbyβ* photometry and found a significant underabundance ([Me/H] = −0.5) for NGC 2451, contrary to Pastoriza & Röpke (1983), who find from DDO photometry of nine red giant stars a metallicity of $[Fe/H] = -0.11\pm0.12$. The latter also proposed a significantly larger age (4.8×10^8 yrs) for the cluster, which relied on several giants. Claria (1985), however, argued that NGC 2451 does not contain any evolved stars.

The first hints that NGC 2451 may actually consist of two different groups of stars at different distances were noted by Maitzen & Catalano (1986) during a search for CP-2 stars in open clusters. However, it was not until kinematic data were introduced by Röser & Bastian (1994) who used proper motions from the PPM catalogue, that the presence of two clusters in the same line of sight could solve that mystery on the discording results derived from previous studies. In particular, they concluded that what was called NGC 2451 is definitely not a cluster, but that there exists a group of 24 stars within a $6^\circ\times6^\circ$ region (called the "Puppis Moving Group") sharing common proper motions and forming a well-defined main sequence at a distance of 220 pc. Due to the presence of B 3 stars the age of the group was constrained to ∼20 Myrs. The possible existence of a second cluster at ∼400 pc distance was concluded from the CMD and the distance modulus histogram. Later on, Platais et al. (1996) claimed to have confirmed the existence of the second cluster.

Based on position, proper motion and parallax measurements by the *Hipparcos* satellite, Baumgardt (1998) found a distance of 190 pc derived from 12 members of the nearer cluster A. He also found hints for the distant cluster B and noted 23 possible members. However, the proper motions of them were indistinguishable from the galactic background.

Table 1. The journal of ROSAT X-ray observations.

Seq.-ID	Detector	Date of Obs.	Obs. dur. (ksec)	Desig.
WG201217p	PSPC	1992–11–12	9.22	A
WG201576p	PSPC	1993–10–10	10.32	B
WG202531h	HRI	1996–11–1-3	57.58	H

Carrier et al. (1999) performed an extensive study of the brighter stars (B-, A-, early F-types) of the cluster by means of proper motions, parallaxes and Geneva photometry for 64 stars. Although their study was primarily focussed on the analysis of a specific Be star in that region, they proposed to have confirmed the existence of both clusters and identified 32 stars as members of cluster A, 13 stars as members of cluster B and 19 stars as non-members. They derived distances of 197 ± 12 pc and 358 ± 22 pc, respectively, and the same age for both clusters of 50 Myrs. The distance to cluster A based on *Hipparcos* parallaxes was also computed by Robichon et al. (1999) to 188.7 (+7.0/−6.5) pc.

Recently, a comprehensive study of NGC 2451 A including CCD *BV* photometry, proper motions, and high-resolution spectroscopy has been performed by Platais et al. (2001) in the course of the WIYN open cluster project. They identified about 70 stars as probable main-sequence members and derived from an isochrone fit a distance of 189 pc and an age of 60±20 Myrs.

3. X-ray observations

3.1. Observations and data reduction

The ROSAT X-ray observations were carried out at three different epochs between 1992 and 1996. Two PSPC (called "A" and "B") and one HRI ("H") observations were scheduled on NGC 2451, the details are listed in Table 1. All of these pointings were centered on the bright star c Pup (RA = $07^{\rm h}45^{\rm m}15^{\rm s}$, Dec = $-37^\circ\,58'\,06''$ (2000.0)), at that time supposed to be close to the cluster center. A short overview on the X-ray observations of NGC 2451 was already given by Hünsch (2000) and Hünsch & Weidner (2002).

The PSPC covers a circular field of view of ∼2° diameter and has a coarse spectral resolution of $E/\Delta E \approx 2$ at 1 keV. The HRI has a smaller rectangular field of view ($36' \times 36'$) and a higher spatial but no spectral resolution.

For the data analysis, we used standard EXSAS routines, details can be found in Weidner (2000). In order to increase the sensitivity of the PSPC observations we also created a further artificial pointing called "C" by merging pointings A and B. The source detection for the PSPC pointings A, B, and C was performed in three different energy bands separately, i.e., a broad band (0.1–2.4 keV), a soft band (0.1–0.5 keV), and a hard band (0.6–2.1 keV). If an X-ray source is detected in both the soft and the hard band, the hardness ratio $hr = (H-S)/(H+S)$, where H and S denote the count rates in the hard and soft bands, respectively, provides a coarse information on the spectral energy distribution ("X-ray colour"). Since the HRI detector has no intrinsic energy resolution, this procedure could not be applied for pointing H.

For the conversion of count rates into energy fluxes, an emission model dependent energy-conversion factor (ECF) has to be applied. Based on our experience from fitting spectral models to the X-ray emission observed by the ROSAT PSPC we used individual ECFs depending on the hardness ratio (cf. Hünsch et al. 1998). Where the hardness ratio could not be derived the following mean values for the ECF (in erg cm^{-2} cts^{-1}) are applied, PSPC, cluster members: 8×10^{-12}, PSPC, non-members: 6×10^{-12}, HRI, members: 2.8×10^{-11}, HRI, non-members: 2.1×10^{-11}, the difference for supposed cluster members and non-members resulting from the assumed mean interstellar hydrogen column densities of 5×10^{19} cm^{-2} and 1×10^{19} cm^{-2}, respectively.

The significance of an X-ray source is given by the likelihood parameter Li = $-\ln(1-P)$, where P is the probability of existence. We set the threshold for an accepted X-ray source to Li = 6 which corresponds to a detection at 3σ level. Assuming a typical coronal X-ray emission mechanism, i.e., a Raymond-Smith model with $\log T \approx 6.4$ and a hydrogen column density of $\log N_{\rm H} \approx 21$ the minimum detectable X-ray fluxes in the center of the PSPC field of view are about 9×10^{-15} erg cm^{-2} s^{-1} for pointings A and B, 6×10^{-15} erg cm^{-2} s^{-1} for pointing C, and again 6×10^{-15} erg cm^{-2} s^{-1} for pointing H. Given the distances of 206 pc and 370 pc for the clusters NGC 2451 A and B, this corresponds to minimum detectable X-ray luminosities of 5×10^{28} erg s^{-1} in the case of pointings A and B, and 3×10^{28} erg s^{-1} in the case of pointings C and H for the nearer cluster A, and 1.5×10^{29} erg s^{-1} (pointings A and B) and 1.0×10^{29} erg s^{-1} (pointings C and H) for the more distant cluster B.

A point of special concern is the UV sensitivity of the HRI (Zombeck et al. 1997) resulting in a non-negligible contribution of UV radiation to the measured count rate in the case of bright early-type stars. For all such stars (i.e., $V < 9.0$) in our HRI field of view, we cross-checked the X-ray fluxes derived from both PSPC and HRI count rates and found significant differences for the three brightest B-type stars only: for X80 the HRI X-ray flux is about twice as much as the PSPC flux, and X61 and X84 are detected by the HRI only, but not in the PSPC observations. From the calculations given by Barbera et al. (2000) we estimated the UV contamination to the observed HRI count rate to be at maximum 40% in the case of X84 (and even less in the case of the optically fainter X61). That would not explain their non-detections by the PSPC. However, the star's X-ray emission may be variable (see Sect. 3.2.2). For stars fainter than $V \approx 7.5$ the UV contamination is negligible.

3.2. Analysis

3.2.1. X-ray sources

The numbers of detected X-ray sources in the various pointings (whole field of view) and energy bands are given in Table 2.

Since many X-ray sources appear in different pointings and pass bands, a cross check was performed to identify identical

Table 2. Number of detected X-ray sources. For the definition of the energy bands see text.

Pointing	Broad band	Soft band	Hard band
A	105	32	110
B	87	24	100
C	122	35	142
H	87	–	–

sources and to derive averaged positions for them. In particular, we assume sources as identical if they fall within a circle of 25 arcsec (PSPC) or 5 arcsec (HRI), and the final positions are computed as a weighted mean depending to the likelihood parameter, and given enhanced weight to HRI positions.

The final list of X-ray sources within the NGC 2451 area contains 188 X-ray sources, which are numbered consecutively according to decreasing declination. For each of the three ROSAT pointings, we give the list of detected X-ray sources in Tables 3–6, including a list of sources detected only in the merged pointing C. In Tables 7–10 we present the list of X-ray sources identified with stellar counterparts separately for clusters NGC 2451 A and B and the non-members, (see Sect. 5.2), giving the final X-ray position as described above, the positional offset between X-ray source and star, V magnitude and $B-V$ colour. Note that the X-number in the first column corresponds to the number given in the source Tables 3–6. This number serves as a cross reference for all these tables.

3.2.2. Variability

The nature of the ROSAT X-ray observations allows us to study both short-term and long-term variations of the X-ray flux.

Short-term variations can be inferred from the arrival time information given for the individual photons. Since it is not possible to distinguish between source photons and background photons, the individual events have to be summarized into time-bins so that light curves of mean count rates can be constructed. Obviously, this is possible for the stronger X-ray sources only, and for a detailed analysis we set a minimum of 50 counts for PSPC sources and 150 counts for HRI sources. Restricting ourselves to stronger sources, but investigating also different energy bands where possible, we derived altogether 169 light curves. Of these, 4 objects showed significant X-ray flaring; these events are discussed in more detail in Sect. 6.6.

The time basis of about 1 yr between the two PSPC observations and 3 yrs between the second PSPC observation and the HRI observation allows a detailed study of the long-term variations of the X-ray flux.

If we define the significance of X-ray variations between the two PSPC pointings as

$$n_\sigma = \frac{|\mathrm{CR(A)} - \mathrm{CR(B)}|}{\sqrt{\mathrm{ECR(A)}^2 + \mathrm{ECR(B)}^2}},$$

where CR and ECR are the count rates and their errors for pointings A and B, respectively, we find that out of the 83 stars detected in both exposures 16 show variations at more than 2σ level, of which 9 even exceed the 3σ level. Except from the flare objects, the largest variations are by a factor 3 to 5 (X94, X134, X181), but most do not exceed a factor of 2. The stars found to be X-ray variable at $>2\sigma$ level are indicated in Tables 7–10. The individual count rates and X-ray fluxes can be infered from the Tables 3–6. In principle, all spectral types of stars from B-types to M-types do show variations.

The comparison between the PSPC and HRI observations having a time basis of 3–4 years is much more difficult since the different sensitivities, the energy-dependence of the sensitivity, and general calibration uncertainties for the different detectors make the significance of any detected flux variation far more difficult to assess. Notwithstanding these uncertainties we compared the derived X-ray fluxes of 31 sources found in both the HRI and at least one of the PSPC exposures and found that most of the HRI fluxes are in good agreement with the PSPC fluxes, often inbetween the two values derived from both PSPC exposures if these differ considerably (see individual fluxes in Tables 3–6). Except from one case with strong UV contamination (see Sect. 3.1) there is only one X-ray source (X81) which shows a significantly increased X-ray flux in the HRI observation compared to the two PSPC observations.

4. Optical observations

4.1. Observations and data reduction

For the central part of the NGC 2451 region optical $UBVR$ photometry was performed during 5 nights in December 1997 at the ESO 0.9 m Dutch telescope. A Tektronix TK512CB grade 1 chip with 510×510 pixels was used. The pixel size of 27 μm yields a plate scale of 0.44″/pixel at the telescope's Dall-Kirkham focus, thus a field of 3.77×3.77 square arcmin could be imaged. The dimensions of the cluster forced us to spread the images over a grid of 128 fields covering the central part, where most of the X-ray sources are found. Additionally, exposures of Landolt standard stars were taken several times during each night.

Observing conditions were moderate to good, except from some cirrus clouds ocurring during part of three nights. Typical exposure times were 120 s in U, 15 and 90 s in B, and 10 and 60 s in V and R, the shorter times being used for measurements of brighter stars. Unfortunately, the observation time was not sufficient to cover the whole cluster center with R exposures, hence, the R data are incomplete and we refrain from drawing $(V-R)-V$ diagrams.

The data were processed using standard IRAF routines, i.e., bias subtraction and flatfielding by twilight flats. For each field, a plate solution was derived from at least three GSC stars, yielding astrometric positions for the measured stars to about 1 arcsec accuracy. Where not enough guide stars were available, a plate solution could be derived from stars in regions overlapping with neighbouring fields. Only in a few cases of isolated fields this was not possible.

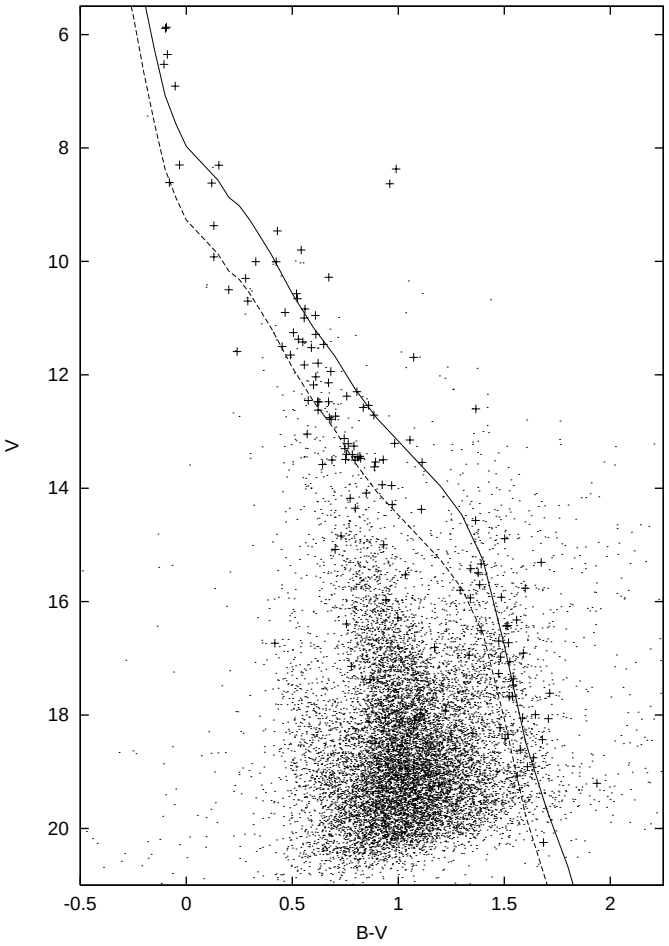

Fig. 1. Colour-magnitude diagram of 13 307 stars measured in our photometry of the central NGC 2451 region. Stars identified with X-ray sources are indicated by crosses. Most of them obviously form a main-sequence-like structure among the brighter stars. The solid and dashed lines indicate the expected locations of main sequences at distances of 197 pc and 360 pc, respectively.

4.2. Optical photometry

Stellar magnitudes are derived by means of both aperture photometry (standard stars, isolated bright stars in short exposures) and PSF fitting photometry. We used the DAOPHOT package (Stetson 1987) as implemented in IRAF. Instrumental magnitudes are converted into calibrated magnitudes by solving the transformation equations in each colour. Zero points, extinction and colour coefficients are derived from photometry of Landolt standard stars that were observed several times during each night at varying zenith distances. Photometric errors are computed quadratically by using standard error propagation.

The magnitudes of altogether 13 307 stars were derived. For stars brighter than 10th mag even the short exposures are overexposed, their magnitudes are taken from the literature as given in SIMBAD. Typical photometric errors are 0.03 in V and 0.02 in B for stars of 12th magnitude, and 0.08 in V for 18th mag stars, mainly dominated by the varying sky transparency due to cirrus clouds. The colour-magnitude diagram of all stars measured is shown in Fig. 1. Relying on photometric data alone a cluster main sequence can hardly be discerned.

5. Identification of cluster members

5.1. Identification of X-ray sources with stars

Starting out from the positions of the 188 X-ray sources we searched for star-like objects within a circle of 25 arcsec radius, i.e., the typical positional uncertainty of the PSPC, around each X-ray position. Not considering the few cases of outlying sources for which we do not have optical data, this gives a total integrated search area of approximately $188 \times \pi\ (25/60)^2 = 102.5$ square arcmin. The mean star density is roughly $13\,307/(128 \times 3.8 \times 3.8) = 7.31$ stars per square arcmin (neglecting the overlap between the CCD images), hence we would expect about 750 possible stellar identification candidates, i.e., typically 4 stars for each X-ray source. Therefore, the search for probable identifications had to be refined and we proceeded in the following way:

First of all, for the 85 HRI sources (45% of all) the positional uncertainty is much smaller (~5 arcsec) yielding a total search area of 1.8 square arcmin and ~13 candidates, which is the maximum expected as spurious identifications among the 65 stars attributed to HRI sources. In almost all cases there was not more than one object within the HRI error circle. For the PSPC sources we generally considered the brightest star within the error circle as the most probable candidate, except for two cases: where a fainter star better fell on one of the supposed main-sequences (see Sect. 5.2) or where a strong source (with large likelihood) located not too far away from the detector center (i.e., within the inner circle of the PSPC support structure) suggested better positional coincidence with a fainter star. In some cases, where among several faint stars within the error circle none could be chosen as more probable than the others, we refrained from any identification. In that way, the detailed examination of all sources resulted in the identification of 147 stars with X-ray sources. The number of spurious identifications can be estimated if we restrict the input sample to stars not too far away from supposed main-sequences, i.e., above a straight line from ($B - V = -0.5$, $V = 8$) to (1.5, 18). Then we retain 1246 stars, and within about 100 PSPC error circles we would expect 36 stars in total. The true number of spurious identifications is very probably lower since it would be unlikely that so many bright stars are just in chance coincidence with X-ray sources.

5.2. Criteria for membership

In Fig. 1 all stars identified with X-ray sources are marked by crosses. Now, a large number of stars close to the expected main sequences of NGC 2451 A and B become evident. This picture becomes even clearer if we restrict to stars identified with HRI sources only, i.e., with very high positional precision and little chance of spurious identification. We therefore conclude that X-ray emission is a powerful criterion to distinguish between cluster members and field stars in the NGC 2451 region. It is evident that many field stars also exhibit X-ray emission, for example, within the clump of stars below the NGC 2451 main sequences around $B - V \approx 1.0$. Hence, X-ray emission alone is not sufficient to identify cluster members.

Table 7. Final list of X-ray sources identified with stars attributed to cluster NGC 2451 A, yielding Williams number (W #), mean X-ray positions (J2000), offset (Δ) between X-ray and optical positions in arcsec, V magnitudes, measured $B-V$ and de-reddened $(B-V)_0$ colour indices. An asterisk indicates values from the literature used for bright stars that are overexposed in our images. Where significant variations in the X-ray flux have been found an X is written into the Var column. Spectral types are given in parentheses if estimated from the colour index. The last column gives a common star designation.

X #	W #	RA	DEC	Δ	V	$B-V$	$(B-V)_0$	Var	$\log L_x$	$\log \frac{L_x}{L_{bol}}$	Spec.	Notes
X3		7 46 09	–37 24 45	48	10.66*	0.52*	0.51		28.88	–4.92	(F8V)	
X11	256	7 45 28	–37 35 41	9	6.91*	–0.05*	–0.06		29.38	–6.01	B9V	HD 63079
X22		7 46 54	–37 43 07	10	16.72	1.52	1.51		29.27	–2.78	(M2V)	
X30		7 44 16	–37 45 59	34	13.15	1.06	1.05		29.04	–3.99	(K4V)	
X31	68	7 45 38	–37 46 39	5	11.46	0.65	0.64	X	29.91	–3.65	(G3V)	CD–37 3870
X32		7 43 55	–37 46 37	6	16.42	1.52	1.51		29.12	–3.05	(M2V)	
X40		7 45 05	–37 48 07	1	15.49	1.38	1.37		28.99	–3.31	(K8V)	
X59		7 46 29	–37 52 37	16	17.36	1.54	1.53		28.99	–2.82	(M2V)	
X61	251	7 45 05	–37 53 16	1	6.53*	–0.11*	–0.12		–	–	B3IV	HD 62991
X63	15	7 43 49	–37 53 46	1	10.57*	0.52*	0.51		29.19	–4.68	(F8V)	CD–37 3823
X72		7 45 16	–37 54 39	2	12.38	0.76	0.75	X	29.74	–3.45	(G8V)	
X80	267	7 46 10	–37 56 01	4	5.87*	–0.09*	–0.10		29.38	–6.54	B7V	HD 63215
X83		7 45 05	–37 56 35	2	15.42	1.34	1.33		28.94	–3.34	(K8V)	
X84	246	7 44 34	–37 56 36	3	5.89*	–0.10*	–0.11		–	–	B7V	HD 62893
X97		7 47 42	–37 58 43	33	11.86*	0.73*	0.72		29.20	–4.22	(G8V)	
X102		7 44 07	–37 59 24	1	16.43	1.51	1.50		29.30	–2.85	(M1V)	
X103	244	7 44 28	–37 59 16	1	8.62*	0.12*	0.11		29.55	–5.06	A3V	HD 62876
X106		7 43 54	–38 00 03	1	12.30	0.81	0.80		29.46	–3.77	(K0V)	
X108		7 46 25	–38 00 09	20	14.57	1.37	1.36		28.82	–3.88	(K8V)	
X109	46	7 44 56	–38 00 18	4	9.80*	0.54*	0.53		28.80	–5.29	(F8V)	CD–37 3853
X114		7 46 24	–38 01 04	11	12.71	0.89	0.88		28.52	–4.65	(K1V)	
X116	50	7 45 02	–38 02 24	4	10.01	0.42	0.41		28.82	–5.22	(F5V)	CD–37 3859
X117		7 48 07	–38 02 10	9	12.54	0.86	0.85		30.06	–3.09	(K1V)	
X128		7 45 05	–38 04 29	0	17.67	1.54	1.53	X	28.94	–2.79	(M2V)	
X132	47	7 44 60	–38 05 43	5	8.30*	0.15*	0.14		29.77	–4.96	A3V	HD 62974
X134	3	7 42 46	–38 05 54	23	10.84*	0.56*	0.55	X	29.42	–4.34	(F8V)	CPD–37 1499
X142	89	7 46 35	–38 06 43	4	10.01*	0.33*	0.32		29.69	–4.37	(F0V)	CD–37 3897
X144		7 43 51	–38 07 06	5	15.92	1.49	1.48		29.36	–2.93	(M1V)	
X149	94	7 46 49	–38 08 50	15	9.46*	0.43*	0.42		29.27	–5.04	(F5V)	CD–37 3902
X151		7 43 06	–38 09 19	3	15.34	1.39	1.38	X	29.65	–2.73	(M0V)	
X152		7 45 22	–38 09 51	39	13.21	0.98	0.97		28.52	–4.49	(K3V)	
X156	57	7 45 15	–38 11 50	3	11.00	0.56	0.55	X	30.31	–3.38	(F8V)	CD–37 3862
X157	233	7 43 43	–38 12 14	10	6.35*	–0.09*	–0.10		29.19	–6.51	B9Vsp	HD 62712
X160		7 47 04	–38 12 31	10	16.32	1.56	1.55		29.38	–2.93	(M3V)	
X173		7 43 52	–38 16 20	20	14.89	1.50	1.49		29.58	–3.15	(M1V)	
X177		7 48 15	–38 22 35	48	11.29	0.61	0.60		30.27	–3.32	(G0V)	
X181		7 43 58	–38 27 48	25	13.55	1.11	1.10	X	29.61	–3.21	(K4V)	
X187		7 45 50	–38 33 55	38	12.58	0.84	0.83		29.81	–3.31	(K0V)	
X188		7 44 25	–38 35 49	22	10.95*	0.61*	0.60	X	30.09	–3.64	(G0V)	

Notes on individual objects:
X61: HRI detection only; UV contamination assumed.
X63: probably non-member due to lower metallicity (Hünsch et al. 2003).
X84: HRI detection only; UV contamination assumed.
X109: possibly foreground star; soft X-ray source, slightly above the main sequence, lower Li abundance (Hünsch et al. 2003).
X128: flare star; X-ray parameters given for quiescent state.
X151: flare star; X-ray parameters given for quiescent state.
X156: close visual binary, not resolved in X-rays.
X177: close visual binary, not resolved in X-rays.

Using the distances and thus the location of the NGC 2451 main sequences from the literature, we used the proximity to the expected main sequences as an additional criterion for cluster membership. In particular, for each of the two main sequences we selected all stars within an envelope of 0.75 mag above the main sequence (i.e., allowing for equal-mass binaries) and within the photometric measurement errors below and above that strip.

Table 8. Same as Table 7, but for cluster NGC 2451 B.

X #	W #	RA	DEC	Δ	V	$B-V$	$(B-V)_0$	Var	$\log L_x$	$\log \frac{L_x}{L_{bol}}$	Spec.	Notes
X7		7 45 34	–37 30 29	37	12.73	0.70	0.65		30.34	–3.21	(G5V)	
X12	18	7 43 58	–37 37 15	12	12.14	0.67	0.62		30.03	–3.76	(G2V)	
X15	243	7 44 28	–37 39 50	2	8.30*	–0.03*	–0.08	X	30.01	–5.46	B8V	HD 62875
X16	41	7 44 52	–37 40 13	15	10.70*	0.29*	0.24		28.92	–5.40	(A8V)	CD–37 3850
X17		7 45 09	–37 41 30	7	14.29	0.97	0.92		29.74	–3.28	(K2V)	
X27	69	7 45 42	–37 44 33	5	11.26	0.51	0.46	X	30.14	–3.83	(F5V)	CD–37 3871
X29		7 45 12	–37 45 11	6	13.30	0.75	0.70		29.69	–3.65	(G8V)	
X33		7 44 29	–37 46 46	3	12.76	0.68	0.63		29.67	–3.87	(G2V)	
X39		7 45 35	–37 47 59	31	12.45	0.58	0.53		29.45	–4.39	(F8V)	
X42		7 47 26	–37 48 19	4	11.50	0.45	0.40		30.37	–3.64	(F5V)	CD–37 3910
X45	61	7 45 21	–37 49 52	2	11.83	0.56	0.51		29.69	–4.20	(F8V)	CPD–37 1565
X50		7 45 29	–37 51 23	1	13.51	0.80	0.75		29.81	–3.46	(G8V)	
X56		7 45 54	–37 51 50	11	16.51	1.39	1.34		29.40	–3.02	(K8V)	
X57		7 45 34	–37 51 53	2	13.45	0.81	0.76		29.54	–3.74	(G8V)	
X60		7 44 23	–37 52 55	1	13.26	0.79	0.74		30.31	–3.05	(G8V)	
X64		7 46 09	–37 53 48	6	15.80	1.29	1.34	X	29.70	–2.99	(K8V)	
X65		7 45 46	–37 53 49	2	13.22	0.76	0.71		29.73	–3.64	(G8V)	
X66		7 45 21	–37 53 58	1	13.95	0.97	0.92	X	29.68	–3.47	(K2V)	
X68		7 44 36	–37 54 02	1	13.40	0.76	0.71	X	30.17	–3.13	(G8V)	
X74		7 44 10	–37 54 53	1	13.41	0.78	0.73		30.07	–3.23	(G8V)	
X81		7 43 25	–37 56 04	10	13.48	0.82	0.77	X	29.59	–3.69	(G8V)	
X88		7 42 60	–37 57 24	11	12.48	0.63	0.58		29.78	–3.87	(G0V)	
X93	16	7 43 50	–37 58 06	10	9.92*	0.13*	0.08		29.32	–5.13	A2V	CD–37 3825
X94	254	7 45 15	–37 58 06	1	3.64*	1.72*	1.67	X	29.78	–8.72	K2.5Ib-II	HD 63032=c Pup
X96		7 45 59	–37 58 39	5	13.54	0.89	0.84		29.82	–3.47	(K0V)	
X101	22	7 44 08	–37 59 06	9	9.37*	0.13*	0.08		30.05	–4.81	B9V	HD 62802
X105	48	7 45 01	–38 00 02	2	11.65	0.49	0.44		29.91	–4.04	(F5V)	CPD–37 1549
X107	54	7 45 10	–38 00 05	2	11.37	0.53	0.48		29.83	–4.25	(F5V)	NSV 3722
X110	124	7 44 33	–38 00 28	0	11.80	0.62	0.57		30.39	–3.52	(G0V)	
X111		7 44 19	–38 00 21	2	14.37	1.11	1.06		29.68	–3.33	(K4V)	
X112	76	7 46 02	–38 00 30	4	12.04	0.61	0.56		29.34	–4.49	(F8V)	CPD–37 1582
X115		7 45 03	–38 01 54	1	12.48	0.62	0.57		30.32	–3.33	(G0V)	
X119	2	7 42 45	–38 03 11	31	10.30*	0.28*	0.23		29.76	–4.71	(A8V)	CD–37 3810
X120		7 48 14	–38 02 56	24	12.62	0.62	0.57		29.65	–3.93	(G0V)	
X127		7 45 56	–38 04 06	8	16.95	1.33	1.28		29.92	–3.26	(K7V)	
X131		7 43 18	–38 05 43	29	13.12	0.75	0.70		29.64	–3.77	(G5V)	
X133		7 44 49	–38 05 57	2	13.49	0.75	0.70		29.34	–3.94	(G8V)	
X137		7 45 04	–38 06 09	5	12.79	0.68	0.63		30.00	–3.52	(G2V)	
X139	266	7 46 13	–38 06 11	30	8.61*	–0.08*	–0.13		29.55	–5.85	A0IV	HD 63216
X145		7 44 51	–38 08 01	2	13.62	0.89	0.84		29.62	–3.62	(K0V)	
X150		7 45 46	–38 09 12	5	13.50	0.93	0.88		30.08	–3.23	(K1V)	
X154	8	7 44 43	–38 11 03	2	13.94	0.92	0.87		29.71	–3.44	(K1V)	
X155	66	7 45 28	–38 11 32	21	11.42*	0.55*	0.50		29.30	–4.76	(F8V)	CD–37 3869
X158		7 45 09	–38 12 11	20	15.94	1.34	1.29		29.74	–2.85	(K7V)	
X161		7 46 12	–38 12 37	3	13.44	0.82	0.77		29.83	–3.47	(G8V)	
X167	35	7 44 39	–38 13 44	30	10.50*	0.20*	0.15		29.34	–5.07	(A5V)	CD–37 3843
X172	51	7 45 02	–38 14 51	4	12.48	0.67	0.62		30.04	–3.63	(G2V)	
X180	118	7 45 03	–38 26 24	53	12.18*	0.60*	0.55		29.42	–4.35	(F8V)	
X186	283b	7 47 27	–38 31 01	26	10.90*	0.47*	0.42		29.84	–4.41	F2V	HD 63465 B

Our final list of probable cluster members contains 39 stars of cluster NGC 2451 A, 49 stars of NGC 2451 B, and 22 faint stars, the photometric errors of which are so large that they cannot be attributed to a certain cluster, yet they are probably members of one of the two clusters. 40 stars identified with X-ray sources are classified as non-members (see Tables 7–10). Bolometric corrections for the calculation of normalized X-ray luminosities were taken from Johnson (1966) according to the de-reddened $(B-V)_0$ colours of the stars.

Note the significant gap on both main sequences in the $B-V$ range 1.0 to 1.3, i.e., K-type dwarfs. This gap is probably related to a locally steeper gradient in the mass-colour relation and was also found by Randich et al. (1996b) in the case of the α Per cluster.

Table 9. Same as Table 7, but for faint stars probably members of either of the two cluster, yet not known to which because of large errors in $B-V$. For the calculation of bolometric fluxes dependent on apparent magnitude and de-reddened colour, we assumed an average reddening of $E(B-V) = 0.05$.

X #	W #	RA	DEC	Δ	V	$B-V$	$(B-V)_0$	Var	$\log \frac{L_x}{L_{bol}}$
X4		7 42 10	–37 26 47	25	18.23	1.48	1.43		–1.41
X34		7 44 17	–37 47 14	10	18.42	1.50	1.45		–2.41
X35		7 43 13	–37 47 21	25	15.70	1.38	1.33		–2.80
X36		7 44 35	–37 47 28	4	17.62	1.71	1.66		–3.22
X37		7 45 13	–37 47 30	8	17.99	1.65	1.60		–2.83
X38		7 44 49	–37 47 49	1	18.43	1.68	1.63		–2.80
X41		7 44 44	–37 48 08	6	18.06	1.71	1.66		–3.02
X44		7 44 37	–37 49 02	5	16.70	1.47	1.42		–2.78
X49		7 45 33	–37 51 23	3	17.68	1.52	1.47		–2.39
X71		7 44 18	–37 54 17	15	18.62	1.58	1.53		–2.89
X73		7 45 36	–37 54 49	12	16.91	1.59	1.54		–3.25
X76		7 44 37	–37 55 00	3	17.06	1.53	1.48		–3.26
X82		7 45 47	–37 56 19	4	18.75	1.64	1.59		–3.01
X86		7 44 26	–37 56 58	3	18.34	1.52	1.47		–2.38
X87		7 45 10	–37 57 12	2	19.08	1.56	1.51		–2.66
X91		7 46 02	–37 57 47	4	17.47	1.54	1.49		–3.23
X113		7 45 27	–38 00 53	5	18.91	1.61	1.56		–2.84
X121		7 44 36	–38 02 58	2	18.05	1.59	1.54		–3.03
X124		7 43 45	–38 03 56	6	20.25	1.69	1.64		–1.95
X126		7 45 23	–38 04 09	2	19.21	1.94	1.89		–3.24
X130		7 46 02	–38 04 44	15	16.98	1.48	1.43	X	–2.78
X136		7 45 29	–38 05 50	2	17.27	1.47	1.42		–2.49

5.3. Comparison of X-ray based cluster membership with other methods

Carrier et al. (1999) list 32 stars as probable members of NGC 2451 A, most of them B- and A-type stars of known proper motion and parallax, while for 14 stars only photometric data exist. Since these early-type stars are not expected to show up in X-rays unless they have a late-type companion, little can be stated from a comparison between their and our membership lists. Still, of the 20 stars of their sample located in the PSPC field of view, we find 10 stars as X-ray sources, and of the 13 stars attributed by Carrier et al. to NGC 2451 B, 7 of which are covered by our X-ray observations, we find 3 stars in our list of cluster B.

Platais et al. (2001) have carried out a detailed photometric and proper motion study of an extended field around NGC 2451. They identified 136 possible members of cluster A down to B magnitude 15 by means of proper motion and found the center of cluster NGC 2451 A to be at RA = $07^h\ 43\overset{m}{.}3$, Dec = $-38°\ 16'$ (J2000.0), which is about half a degree away from the position originally believed to be the cluster center and chosen as the target of our ROSAT pointings. Therefore, our X-ray data cover only part of the supposed cluster region in the sky.

Table 11 yields the numbers of probable members found by Platais et al. within the PSPC and HRI fields of view and defines the subsamples that have to be compared with our membership list. This result suggests that only in the central part of the area investigated in X-rays our sensitivity was sufficient to detect the majority of cluster members. The non-detected probable late-type cluster members and upper limits for their X-ray luminosity are given in Table 12.

On the other hand, the photographic plates used for the astrometric study of Platais et al. include the whole PSPC field of view. Of the 113 stars identified by us as optical counterparts of X-ray sources, 58 are also listed by Platais et al. 19 of them are identified as probable NGC 2451 A members of which 18 are also attributed to cluster A by our study. 3 stars are considered as non-members (of cluster A), all of them are attributed by us to cluster B. For 36 stars no proper motion information exists.

Summarizing the cross-check with the Platais et al. study and considering the different sky areas and the different optical magnitude limits we can state that the different approaches of finding NGC 2451 A cluster members by means of either X-ray emission or proper motions lead to quite a satisfying agreement, in spite of the low number of coinciding objects. The majority of probable cluster members according to Platais et al. are not detected in X-rays because they are located outside or in the outer parts of the PSPC field of view. Conversely, many fainter stars showing X-ray emission and attributed to the clusters are too faint to be measurable on the astrometric plates used by Platais et al.

6. Properties of the NGC 2451 clusters

6.1. Interstellar absorption

Using our photometric *UBV* data we constructed $(B-V)$–$(U-B)$ colour-colour diagrams for both clusters. While for NGC 2451 A the X-ray selected probable member stars are located very close to the track for unreddened main-sequence

Table 10. Same as Table 7, but for stars supposed to be non-members of the two NGC 2451 clusters. We assumed a reddening of 0.00 for stars to the right of the two cluster main sequences, 0.05 between the main sequences (X159, X182), and 0.10 to the left of the main sequences.

X #	W #	RA	DEC	Δ	V	$B-V$	$(B-V)_0$	Var	$\log \frac{L_X}{L_{bol}}$	Notes
X2		7 44 13	–37 20 55	5	10.28*	0.67*	0.67	X	–3.37	CD–37 3832
X8	78	7 46 11	–37 31 54	3	11.69	1.07	1.07		3.41	CD–37 3885
X13		7 43 12	–37 37 35	9	15.31	1.67	1.67		–3.38	
X20		7 45 10	–37 42 08	5	18.09	1.08	0.98		–1.40	
X24		7 45 39	–37 44 23	18	17.37	0.87	0.77		–2.28	
X26		7 44 23	–37 44 29	3	14.09	0.85	0.80		–3.39	
X28		7 45 12	–37 44 34	21	13.58	0.64	0.59		–4.05	
X43		7 45 27	–37 48 30	1	13.05	0.57	0.52		–4.50	
X47		7 46 11	–37 50 27	35	14.18	0.77	0.67		–3.73	
X51		7 45 09	–37 51 29	28	14.84	0.73	0.63		–3.65	
X52		7 44 18	–37 51 34	5	18.50	0.89	0.79		–2.37	
X54		7 44 49	–37 51 39	11	16.73	0.42	0.32		–2.74	
X58		7 44 38	–37 52 08	9	18.13	0.86	0.76		–2.36	
X67		7 45 08	–37 53 55	11	16.40	0.76	0.66		–3.28	
X78		7 45 24	–37 55 42	20	16.29	1.00	0.90		–3.52	
X79		7 44 42	–37 55 47	21	17.14	0.78	0.68		–3.29	
X89		7 45 19	–37 57 26	4	18.31	1.35	1.25		–2.54	
X90		7 47 07	–37 57 41	19	15.97	0.94	0.84		–2.85	
X92		7 42 55	–37 57 52	10	17.98	1.11	1.01		–2.17	
X95		7 45 32	–37 58 21	2	18.96	1.07	0.97		–2.06	
X98		7 44 19	–37 58 57	3	15.53	1.03	0.93		–3.54	
X123		7 44 04	–38 03 50	4	16.81	1.17	1.07		–2.76	
X125		7 45 10	–38 04 04	24	15.08	0.70	0.60		–3.55	
X135		7 44 21	–38 06 03	22	12.60	1.37	1.37		–4.84	
X140		7 44 38	–38 06 11	8	18.59	1.27	1.17		–2.33	
X141		7 46 25	–38 06 29	7	19.29	0.94	0.84		–1.66	
X146	238	7 44 04	–38 08 21	20	8.63*	0.96*	0.96		–6.13	HD 62782, G8III
X147	230	7 43 30	–38 08 31	3	8.37*	0.99*	0.96		–5.95	HD 62660, G8III
X148		7 44 26	–38 08 45	27	13.50	0.69	0.64		–3.76	
X153		7 43 09	–38 10 49	26	15.00	0.93	0.83		–3.06	
X159		7 45 53	–38 12 32	12	11.94	0.68	0.63		–4.58	
X162		7 46 20	–38 12 54	3	21.46	0.43	0.33		–0.56	
X163		7 45 37	–38 13 28	7	14.35	0.80	0.70		–3.45	
X164		7 44 46	–38 13 08	8	18.05	0.94	0.84		–2.16	
X166		7 44 42	–38 13 33	9	18.24	1.07	0.97		–2.02	
X170		7 44 37	–38 14 28	4	19.25	1.19	1.09		–0.99	
X171	42	7 44 49	–38 14 24	21	11.59*	0.24*	0.14		–4.90	CD–37 3848
X178		7 46 55	–38 22 42	28	15.77	1.60	1.60		–3.25	
X182	113	7 46 15	–38 27 55	44	11.52*	0.59*	0.54		–4.43	CD–38 3636
X185		7 45 23	–38 30 37	6	17.93	1.22	1.12		–1.65	

stars (Fig. 2), NGC 2451 *B* seems to be considerably reddened. An exact determination is severly hampered by the large scatter, but it seems as if an reasonable fit can be achieved if the assume $E(B-V)$ to be of the order 0.05 (Fig. 3).

For cluster A we therefore confirm the values given by Carrier et al. (1999) and Platais et al. (2001), both of whom give $E(B-V) = 0.01$. For cluster NGC 2451 B, Carrier et al. find a colour excess of $E(B-V) = 0.11$ ($E[B-V] = 0.12$ in the Geneva system), which is based on a few B-type stars only. Our own *UBV* photometry of X-ray selected presumed members of cluster B is shown in Fig. 3, where the magnitudes of the B-type stars are taken from SIMBAD. Contrary to the B-type stars, the A-type stars around $B-V \approx 0.2$ suggest are slighter reddening of $E(B-V) \sim 0.05$. Unfortunately, the large majority of late-type stars does not allow to constrain the reddening much better due to the generally larger measurement errors. As will be shown in the following section, the lower reddening value is also in better agreement with the astrometrically derived distance of 360 pc.

Additional but weak evidence for a stronger reddening of cluster B compared to cluster A comes from the hardness ratios of the X-ray sources. Soft X-ray emission is more absorbed by interstellar hydrogen than hard X-rays. We find that 21 stars attributed to cluster A yield a mean hardness ratio of +0.14 while 6 stars of cluster B give a mean of +0.64.

6.2. Isochrone fitting

Since our study ist concentrated on and mainly expands the known membership among the mid and lower main sequence,

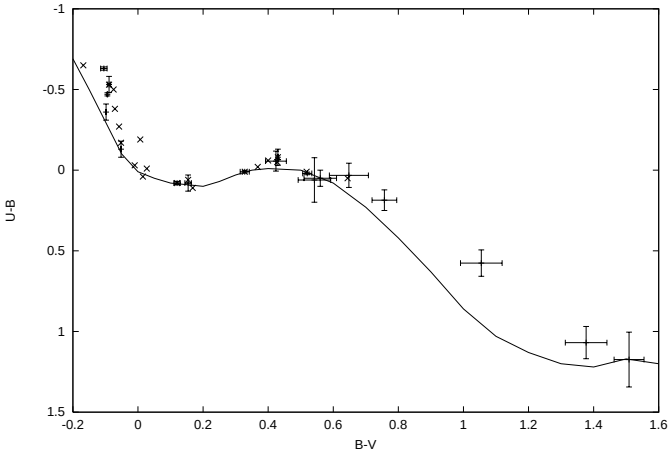

Fig. 2. $(U-B)$–$(B-V)$ two-colour diagram of the stars attributed to NGC 2451 A. The solid line represents unreddened main-sequence stars.

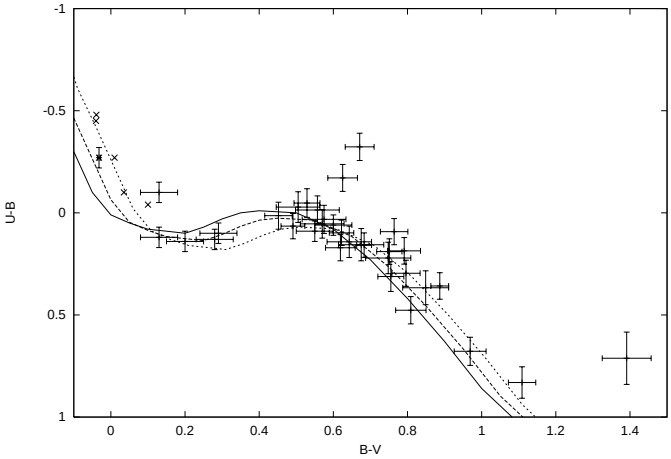

Fig. 3. Same for NGC 2451 B. The solid, dashed, and dotted lines represent the location of main-sequence stars at $E(B-V) = 0.00$, 0.05, and 0.11, respectively.

Table 11. Cross-check of membership derived for NGC 2451 A by Platais et al. (2001) and by our X-ray investigation.

Sample in field of	PSPC	HRI
in field-of-view:	54	14
membership probability >50%:	35	10
B/A-type stars:	10	4
→ late-type stars:	25	6
non-members by our photometry:	3	0
→ comparison sample:	22	6
detected in X-rays:	13	5
percentage:	59%	83%

we do not expect substancial improvements concerning the age of the NGC 2451 clusters based on main-sequence turn-off fitting. Large photometric errors for faint stars and the not extremely young age of NGC 2451 do also not allow an estimate of age based on the settling of low-mass stars onto the main sequence. However, the many late-type stars are well-suited to

Table 12. Probable late-type cluster members based on proper motion (Platais et al. 2001) that were not detected in X-rays.

Platais#	V	$B-V$	$\log L_x$	$\log \frac{L_x}{L_{bol}}$	Notes
987	13.51	1.12	<28.55	<–4.33	
1238	12.75	0.68	–	<–4.63	*
1315	12.30	0.81	<28.95	<–4.27	
1574	14.13	1.17	<29.11	<–3.57	
2223	11.04	0.59	<28.53	<–5.15	
2767	12.11	0.95	<28.76	<–4.59	
3678	11.49	0.67	<28.50	<–5.01	
6567	13.46	1.23			*
6783	14.17	0.67	–	<–3.74	*
6819	13.42	0.88	–	<–4.48	*
8409	13.39	1.06	<28.83	<–4.09	
8422	13.04	1.01	<29.08	<–3.92	

Notes:
#1238: photometry suggests membership of cluster B.
#6567: no X-ray upper limit because too close to X177.
#6783: photometry suggests non-membership.
#6819: photometry suggests membership of cluster B.

constrain the distance which is of course also important for adjusting the main-sequence turn-off and, hence, the cluster age.

A major source of uncertainty in the course of isochrone fitting is the conversion of theoretical parameters (L, $T_{\rm eff}$) into observational parameters ($B-V$, M_V). We therefore compared different stellar evolution codes and different colour transformations with our observational data. In particular, we used the most recent Yale isochrones available from the web (`http://achee.srl.caltech.edu/y2solarmixture.htm`) (Sukyoung et al. 2001) in combination with two different colour transformations (Green et al. 1987; Lejeune et al. 1997), isochrones based on stellar evolution models by Pols et al. (1998; Schröder, private communication), and isochrones by the Padua group (Girardi et al. 2002, `http://pleiadi.pd.astro.it/`).

6.2.1. NGC 2451 A

The distances and ages resulting from the best isochrone fits for NGC 2451 A are listed in Table 13. Examples of isochrone fits are shown in Fig. 4. It is not possible to achieve a good fit to the observed data over the whole range of the main sequence. In general, the Yale g isochrones are slightly too high around $B-V \approx 0.8$, the Yale l isochrones are too high among the early F-type stars ($B-V \approx 0.3$), while the Pols et al. isochrones are too low among the early-type stars. The Girardi et al. isochrones are generally more luminous and thus lead to a slightly larger distance. It is also evident that the Yale isochrones yield a larger age for a good fit of the turn-off point.

In summary, the isochrone fits for NGC 2451 A suggest a distance of 206 ± 10 pc and an age in the range 50 to 80 Myrs, in good agreement with Carrier et al. (1999) and Platais et al. (2001) who used Geneva and Yale isochrones, respectively.

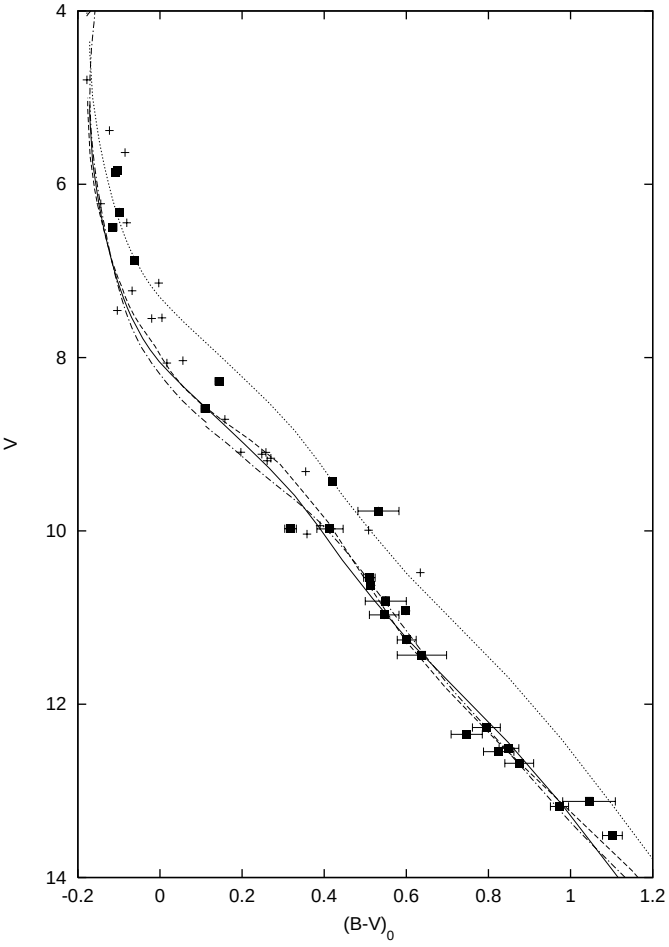

Fig. 4. Isochrone fits for NGC 2451 A using an 80 Myrs Yale isochrone and colour tranformations by Green et al. (solid line) and Lejeune et al. (dashed line) and a 63 Myrs isochrone by Pols et al. (dashed-dotted line). The equal-mass binary envelope is indicated by the dotted line. The stars are de-reddened by $E(B-V) = 0.01$ and adjusted in V magnitude by $A_V = 0.03$. X-ray selected stars are shown as filled squares while additional early-type cluster members from Carrier et al. (1999) are shown as plus signs.

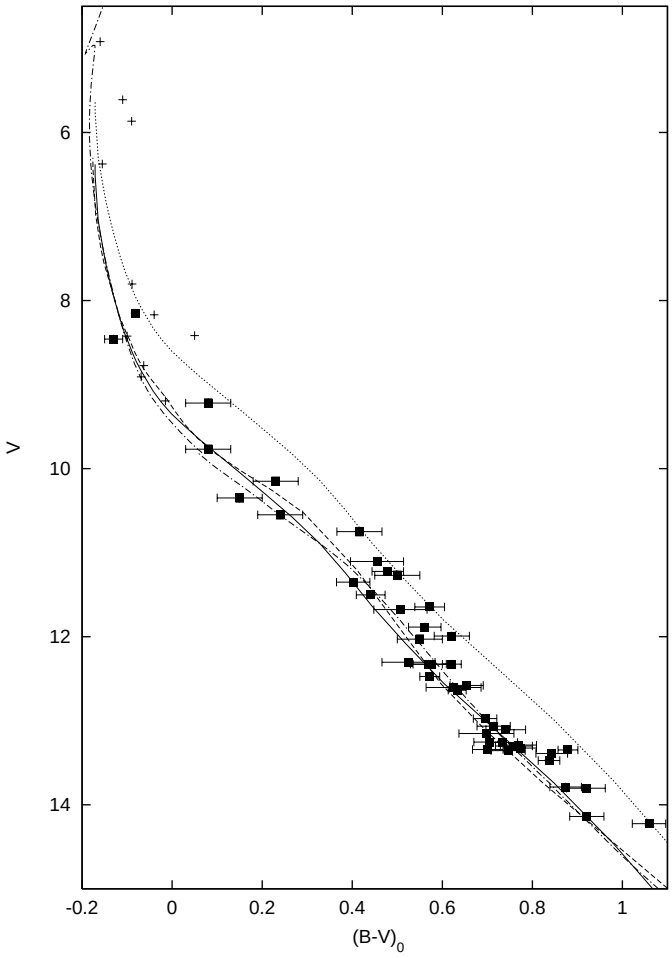

Fig. 5. Isochrone fit for NGC 2451 B using 80 Myrs Yale isochrones and a 50 Myrs isochrone by Pols et al. The line style is similar to Fig. 4.

6.2.2. NGC 2451 B

Assuming a reddening of $E(B-V) = 0.05$ (see Sect. 6.1) the isochrone fitting results for NGC 2451 B are also listed in Table 13. Examples of the fits are shown in Fig. 5. For this cluster, the K-type supergiant c Pup sets an additional data point, which is quite sensitive to age; however, the precise stage of evolution of c Pup is unknown. The Pols et al. isochrones extend to very late stages of evolution, and Fig. 6 shows that 50 Myrs seems to be an upper limit for the cluster's age.

We therefore propose a mean distance value of 370 pc and an age close to 50 Myrs for NGC 2451 B.

Choosing $E(B-V) = 0.11$ as derived by Carrier et al. yields best fits of significantly younger isochrones and an increased distance of ≈450 pc, which is not consistent with astrometric studies.

Table 13. Best fit parameters for different isochrone fits to our observed NGC 2451 colour-magnitude diagrams. Yale g and l denote two different colour transformations (Green et al. 1987 and Lejeune et al. 1997), respectively.

Cluster	Isochrone	distance (pc)	age (Myrs)
NGC 2451 A	Yale g	201	80
NGC 2451 A	Yale l	201	80
NGC 2451 A	Pols et al.	206	63
NGC 2451 A	Girardi et al.	219	56
NGC 2451 B	Yale g	358	80
NGC 2451 B	Yale l	384	80
NGC 2451 B	Pols et al.	366	50
NGC 2451 B	Girardi et al.	380	63

6.3. Detection rate

The fraction of cluster members detected in X-rays is difficult to estimate in the virtual absence of independent methods for identification of cluster members. A quick look at the colour-magnitude diagram (Fig. 1) reveals that the vast majority of stars in the cluster region are background or foreground

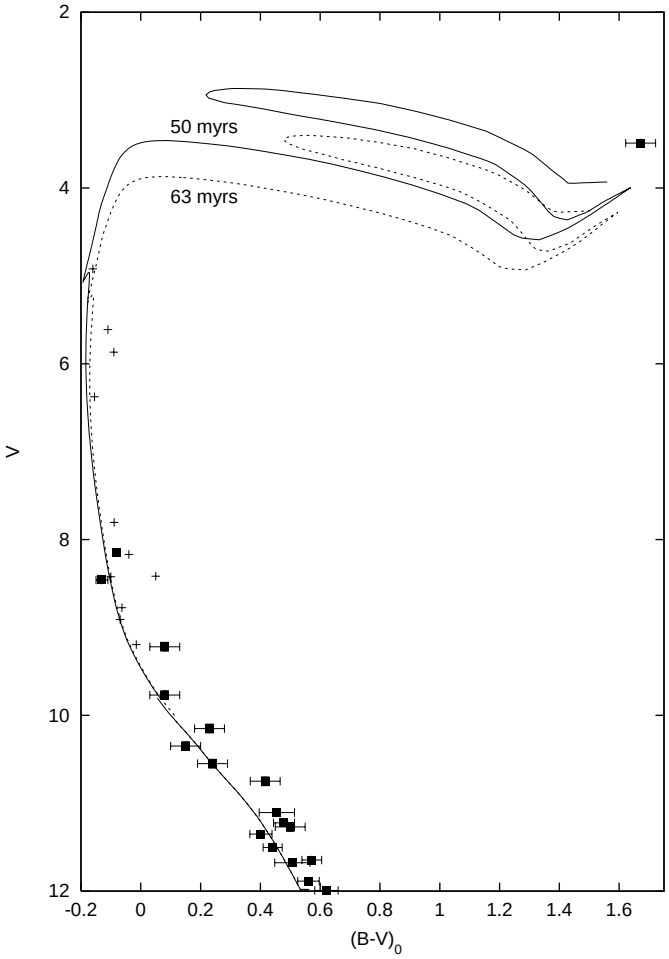

Fig. 6. Isochrone fit for the upper part of the NGC 2451 B CMD. Isochrones by Pols et al. of 50 an 63 Myrs are shown. Note the presence of the supergiant c Pup in the upper right.

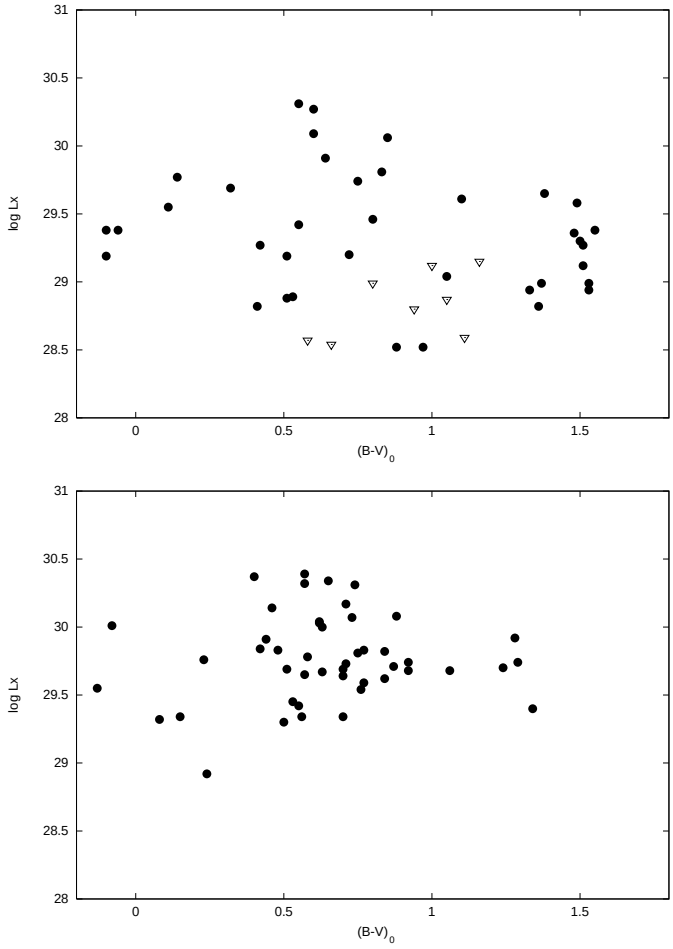

Fig. 7. Distribution of X-ray luminosities vs. $(B-V)_0$ colour of NGC 2451 A (top) and NGC 2451 B (bottom). Detections are shown as filled circles, upper limits as open triangles.

field stars. Restricting ourselves to the upper part of the main sequence, where contamination by field stars is less severe, and also excluding the generally X-ray dark B- and A-type stars, i.e., regarding the region close to the two main sequences of NGC 2451 A and B within the V-magnitude interval 10.0 to 13.0, we find 91 stars. Of these, 36 are detected in the course of our ROSAT observations, yielding a detection rate of 40%. This is quite low compared to the study of α Per by Randich et al. (1996b) who detected 78% of the F-stars and 88% of the G-stars. However, Randich et al. used a pre-selected sample of probable cluster members from proper motion studies, while the 91 stars close to the NGC 2451 main sequences may contain many non-members, which could be located near or between the clusters or distant giants.

As already mentioned in Sect. 5.3, a comparison with the only proper motion study performed for the mid part of the main sequence of NGC 2451 A by Platais et al. (2001) leads to a detection rate in X-rays of 59% considering the whole PSPC field of view and 83% within in inner central region. So, we can assume that in the latter case we achieved a sufficiently deep sensitivity, while in the outer parts we probably have missed a significant fraction of cluster members. This holds at least for the F-, G-, and early K-type stars. We cannot make a statement on the fraction of detected M-type dwarfs since these are too faint to be identified by proper motion studies, yet.

6.4. X-ray luminosities

In Fig. 7 we plot the X-ray luminosities of the stars of both clusters vs. $(B-V)_0$ colour. We computed mean values from the three different pointings and excluded the four flare dominated luminosities (cf. Sect. 6.6). As can be seen, the largest X-ray luminosities as well as the largest scatter in X-ray luminosities occur at the G-type stars. In cluster A, these stars span a range of almost 2 dex, which reduces to 0.8 dex among the M-type dwarfs. The scatter seems to be smaller in cluster B, yet this is probably an artificial result due to the higher detection threshold. We also see a number of A- and late B-type stars in cluster A around $\log L_x \sim 29.5$.

In marked contrast to cluster A, there is a strange lack of K- and M-type dwarfs below the saturation limit ($\log L_x \sim 29.7$) in cluster B although the detection limit would have allowed to find stars about 0.5 dex below that value. This is even more puzzling as we assume the supposed cluster center to be located within the PSPC field of view.

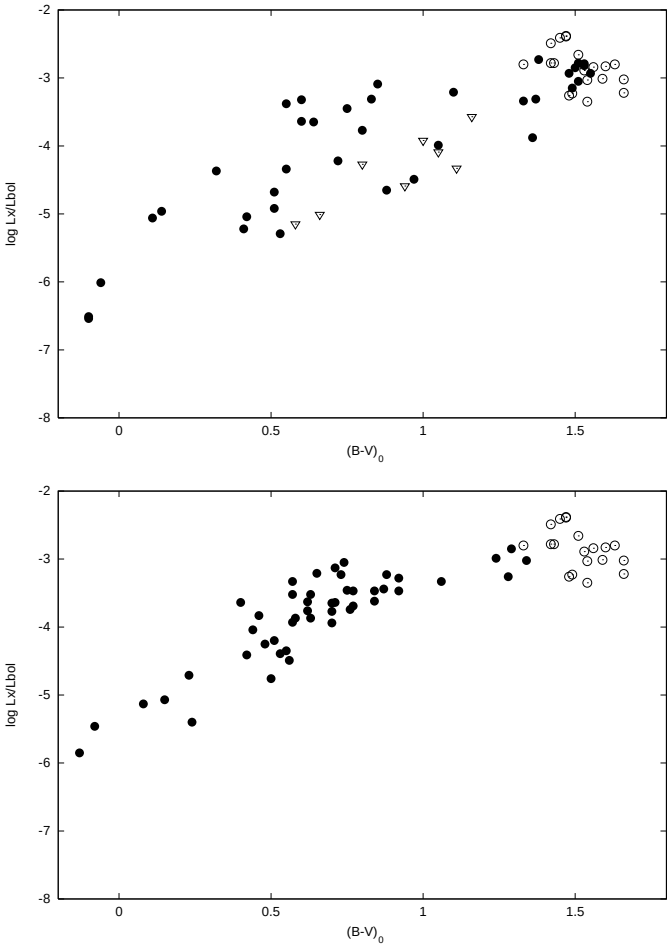

Fig. 8. Distribution of normalized X-ray luminosities L_x/L_{bol} vs. $(B-V)_0$ colour of NGC 2451 A (top) and NGC 2451 B (bottom). Detections are shown as filled circles, upper limits as open triangles, and faint probable members of either of the two clusters as open circles.

Figure 8 shows the normalized X-ray luminosities $\log L_x/L_{bol}$ vs. $(B-V)_0$ colour. Again, the scatter seems to be larger in cluster A than in B. Note that most of the X-ray sources identified with faint stars of unsecure cluster attribution (see Table 9) fit nicely into the diagram, i.e., have normalized X-ray luminosities close to the saturation limit as expected for M-type dwarfs.

6.5. The supergiant c Pup

A remarkable fact is the existence of a very bright supergiant (c Pup = HR 3017 = HD 63032, K 5 Ib-II, X94) which, according to its parallax, proper motion, and radial velocity, is very likely a member of the more distant cluster NGC 2451 B. This star was already identified as a strong X-ray source by Reimers et al. (1996) who also noted the surprising decrease in X-ray luminosity by a factor of 3 within one year. c Pup is known from IUE observations to have an early-type companion (Groote & Reimers 1983), but it is unlikely that the late B- or early A-type star could be the source of the observed X-ray emission. Note that Hünsch & Reimers (1993) have analyzed the UV spectra of c Pup and found the colour excess to be $E(B-V) = 0.04$ in good accordance with the value derived for NGC 2451 B from the colour-colour diagram (see Sect. 6.1). The supergiant c Pup is a very luminous example of the hybrid stars, which are characterized by the simultaneous presence of cool dense winds and hot coronal plasma, thus violating the simple picture of a sharp dividing line in the HRD (see, e.g., Hünsch & Schröder 1996).

Table 14. Characteristic data of the four X-ray flares that occurred during PSPC pointing A. Given are the decay time, the peak X-ray luminosity at the observed maximum, and the whole released energy in the X-ray range integrated over the observed time of the flare.

Source (Cluster)	Sp.type	t_{decay} (sec)	$L_{x,max}$ (erg s^{-1})	E_x (erg)
X128 (A)	(M2V)	5350	1.1×10^{31}	5.9×10^{34}
X151 (A)	(M0V)	7105	7.9×10^{30}	5.6×10^{34}
X27 (B)	(F5V)	≈22 330	5.9×10^{30}	12.6×10^{34}
X74 (B)	(G8V)	≈21 460	2.5×10^{30}	5.4×10^{34}

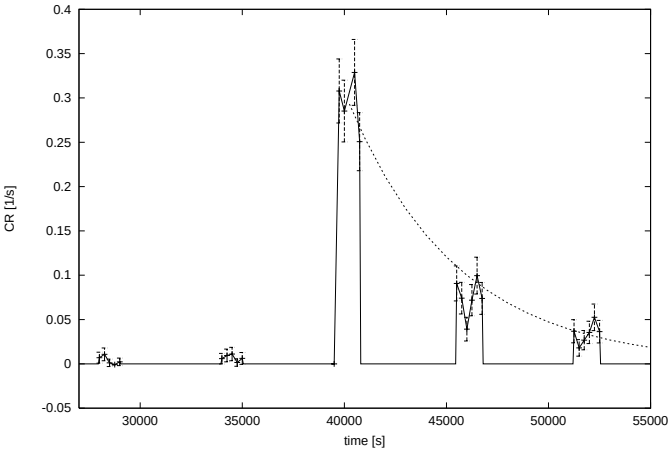

Fig. 9. Light curve of X-ray flare observed during PSPC pointing A on the M-type dwarf associated with X128.

6.6. X-ray flares

During the first PSPC observation (pointing A) four strong X-ray flares occurred in sources which can all be attributed to stars of clusters NGC 2451 A and B. Curiously, no flares were found in the light curves of pointings B and H. The main properties of the flares are given in Table 14.

Two M-type dwarfs of cluster A (X128 and X151) showed significant X-ray flares. The light curve of X128 (see Fig. 9) extends over several observation intervals (OBIs), most of them showing the source in quiescense (at $L_x \approx 1.8 \times 10^{29}$ erg s^{-1}), while the flare and its decay can be nicely followed through the last three OBIs. The actual maximum may have occurred between the fourth and third last OBIs and thus may have been missed. The observed peak count rate is about 60 times higher than the quiescent count rate. A least-square fit of an exponential law yields a decay time of 5.35 ksec. Sufficient counts could be collected to obtain a pulse-height spectrum which could be fitted by a 2T Raymond-Smith model, yielding temperatures

Table 15. Comparison of mean and median X-ray luminosities for NGC 2451 A and B and other clusters of similar age, i.e., α Per and Pleiades (Prosser et al. 1996) and NGC 6475 (Prosser et al. 1995). The log L_x values are given separately for F-type stars ($0.31 \le (B-V)_0 < 0.59$), G-type stars ($0.59 \le (B-V)_0 < 0.82$), K-type stars ($0.82 \le (B-V)_0 < 1.41$), and M-type stars ($(B-V)_0 > 1.41$). The values in parentheses indicate the number of stars used. Note that in the case of NGC 6475 the colour intervals are slightly different and that the K-type stars are divided into early types (upper values) and late types (lower values).

	F stars		G stars		K stars		M stars	
Cluster	mean	median	mean	median	mean	median	mean	median
NGC 2451 A	29.62 ± 0.28	29.23 (8)	29.91 ± 0.14	29.83 (6)	29.49 ± 0.18	29.02 (10)	29.29 ± 0.08	29.29 (8)
(incl. upp.lim.)		29.23 (8)		29.46 (9)		<28.99 (15)		29.29 (8)
NGC 2451 B	29.97 ± 0.11	29.81 (14)	29.95 ± 0.08	29.82 (16)	29.77 ± 0.06	29.71 (11)	–	–
α Per	29.67 ± 0.11	29.59	29.70 ± 0.10	29.68	29.59 ± 0.07	29.62	29.05 ± 0.04	28.98
Pleiades	29.34 ± 0.08	29.33	29.37 ± 0.11	29.21	29.33 ± 0.06	29.38	28.98 ± 0.04	28.99
NGC 6475	29.32 ± 0.07	29.25	29.45 ± 0.05	29.44	29.57 ± 0.08 29.39 ± 0.06	29.64 29.33	–	–

of 1.9 ± 0.4 and 23.1 ± 17.5 MK, the latter value barely constrained due to the limited ROSAT energy range. We performed a coarse analysis of the flare following Schmitt (1994) and using a quasistatic cooling loop model according to van den Oord & Mewe (1989). We derived a lower limit of the density of the flaring plasma of $n_e = 1.2 \times 10^{11}$ cm^{-3}.

The flare on X151 was unfortunately partly obscured by the PSPC support structure, yet it is without question that the flare indeed occurred. One of the OBIs covered the rapid rise of the flare, but the decay time can only roughly be estimated (7.1 ksec). The spectral analysis yields 2T Raymond-Smith model plasma temperatures of 1.9 ± 0.6 and 15.3 ± 1.7 MK, and the derived plasma density is $n_e = 5 \times 10^{10}$ cm^{-3}.

The two X-ray flares that occurred in stars of cluster B (X27 and X74) reached a lower peak flux and had a longer duration. They did not provide sufficient counts for a spectral analysis. Also the decay times could only be estimated very roughly to about 22 ksec, leading to quite large integrated energy releases.

In general, the X-ray flares observed in NGC 2451 A and B are not unusual for young active stars (cf., e.g., Table 1 in Hünsch & Reimers 1995).

7. Comparison with other clusters

In view of the rather young age of the clusters NGC 2451 A and B (cf. Sect. 6.2) it is worthwhile to compare their X-ray properties with those of other similarly-aged and well-investigated clusters, in particular the Pleiades and α Per. Using traditional methods, i.e., location of the main-sequence turn-off, for the Pleiades an age of about 70 Myrs is generally stated while α Per is usually considered to be slightly younger, i.e., 50 Myrs. Both of these nearby (120 and 170 pc, respectively) clusters are very well-studied with extensive membership lists based on proper motions, photometry and parallaxes. Numerous studies have been performed for the Pleiades with the *Einstein* and ROSAT observatories, while the α Per cluster has been investigated mainly by Randich et al. (1996b) and Prosser et al. (1996). NGC 6475 is considered to be significantly older (220 Myrs), yet its cluster members (except from the early and F-type stars) are selected by X-ray emission (Prosser et al. 1995) as was done in our NGC 2451 study. Despite the smaller numbers of known members of the NGC 2451 clusters we can perform a meaningful comparison of the mean and median X-ray luminosities of these clusters, which is given in Table 15.

7.1. NGC 2451 A

The X-ray luminosities generally show a large scatter, except from the M-type stars. Large discrepancies between mean and median values indicate that a few very X-ray luminous or weak stars dominate the means. In particular, the three upper limits among the G-type stars are much below the detections and span an overall range in L_x of about 2 dex, and the K-type stars are somehow underluminous in X-rays compared to the other clusters.

In Fig. 10 we plot the normalized X-ray luminosities for NGC 2451 A in comparison with α Per and the Pleiades. The average activity level of NGC 2451 A seems to be lower than in α Per and roughly comparable with the Pleiades. The saturation limit of $\log L_x/L_{bol} = -3$ is not reached as clearly as for α Per ($B-V \approx 0.6$) or the Pleiades ($B-V \approx 0.75$). Instead, except from the M-type dwarfs, the most active stars remain closely below the saturation limit.

However, whether these subtle differences between the average X-ray luminosities of the clusters are real is questionable. In addition to the uncertainties resulting from the cluster member selection processes, different energy conversion factors and different interstellar extinction may introduce additional possible sources of error.

7.2. NGC 2451 B

Regarding the values given in Table 15 the X-ray luminosities of NGC 2451 B show much less scatter and are generally larger than in NGC 2451 A. The mean and median values for all subclasses of stars (there are no M-type dwarfs detected) are even higher than in α Per. However, as there are no upper limits known in the absence of an independent input sample, this may introduce a strong bias towards active stars. Figure 11 suggests that the average normalized X-ray luminosities of NGC 2451 B are comparable to α Per but also to the high-luminosity tail of the Pleiades.

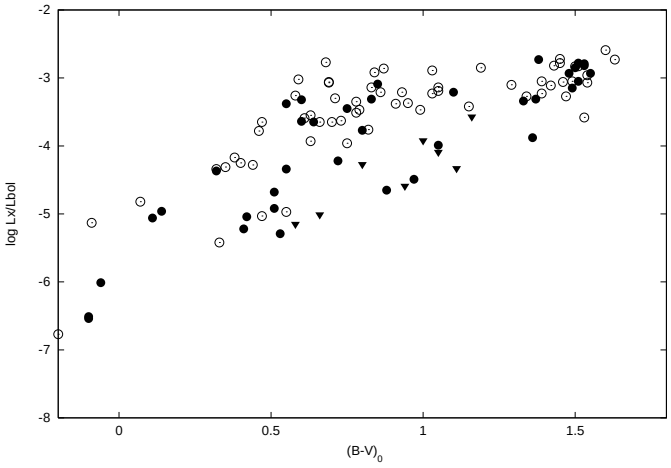

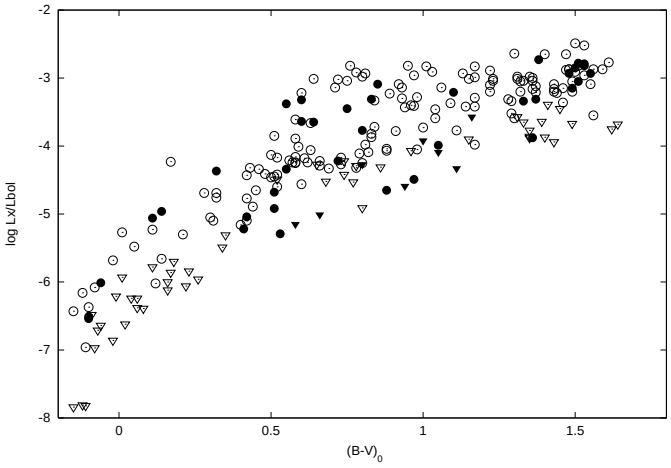

Fig. 10. Comparison of normalized X-ray luminosities $\log L_x/L_{bol}$ vs. $(B-V)_0$ colour of NGC 2451 A with the α Per cluster (top) and the Pleiades (bottom). NGC 2451 A stars are shown as filled symbols, stars of the other clusters as open symbols. Triangles denote upper limits. Pleiades data are from Stauffer et al. (1994), α Per data are from Prosser et al. (1996).

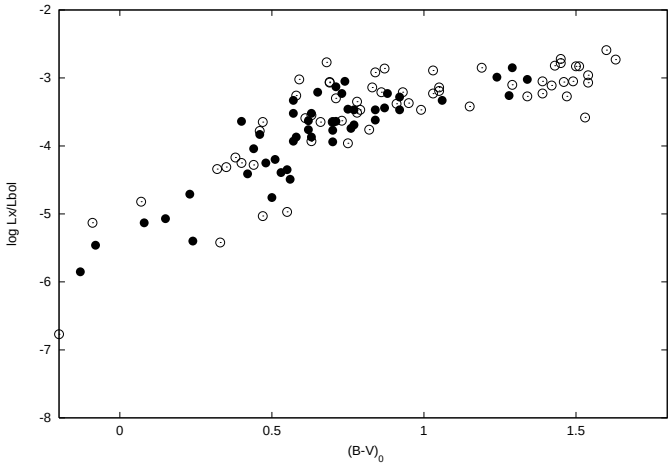

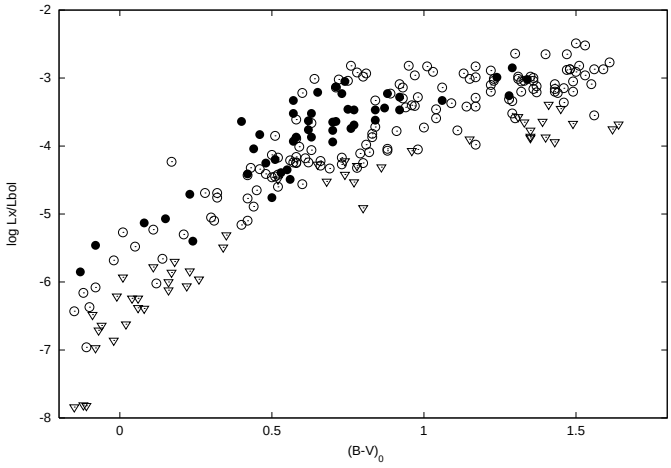

Fig. 11. Same as Fig.10 but for NGC 2451 B.

8. Conclusions

We have performed the first detailed X-ray study of the two young clusters NGC 2451 A and B. In combination with our own optical photometry we were able to identify probable cluster members by means of their X-ray emission and thus to study the main-sequence population down to the M-type dwarfs. The existence of the two clusters is out of question. On the basis of isochrone fits to the observed colour-magnitude diagrams we derived ages and distances for the two clusters.

NGC 2451 A is located at a distance of 206 ± 10 pc and has an age between 50 and 80 Myrs. According to previous astrometric studies, the cluster's center seems to be half a degree away from the field of view centers of our ROSAT PSPC and HRI pointings, and the whole cluster region may actually extend over several degrees. Therefore, our observations cover only part of the cluster. We have found 39 probable members of cluster A on the basis of their X-ray emission. Due to its proximity (NGC 2451 A ranks among the ten nearest clusters), the sensitivity of our X-ray observations is quite good and yield a detection limit of $\log L_x \approx 28.5$. From a comparison with membership lists resulting from different approaches, we are confident to have detected the majority of F- and G-type stars within the X-ray field of view, while our survey is probably incomplete among the K- and M-type stars.

NGC 2451 B has a distance of 370 ± 20 pc and may be somewhat younger (≈50 Myrs) than NGC 2451 A. The cluster seems to be slightly reddened ($E(B-V) = 0.05$). Except from a few early-type stars no detailed astrometric study and, hence, no membership lists exist for this cluster, yet. Our X-ray study revealed 49 stars as probable cluster members on the basis of their X-ray emission. In spite of the higher detection limit due to the larger distance, we have found more X-ray sources in cluster B than in cluster A. We therefore assume that the cluster's center is covered by our X-ray observations, which may be indicated also by the cluster's most massive star, the K-type supergiant c Pup.

We have identified additional 22 X-ray sources with faint stars close to the cluster's lower main sequences, and suggest that these stars are actually M-type dwarf members. Their large photometric measurement errors prevents us from attributing them to one of the two clusters, but their normalized X-ray luminosities close to the saturation limit indicates that theses stars are indeed cluster member candidates.

The X-ray luminosity distribution functions of both clusters are roughly comparable with the ∼similarly-old Pleiades

and α Per clusters, although slight differences seem to exist. NGC 2451 A exhibits a very large scatter in X-ray luminosities and may be more comparable to the Pleiades than to α Per, suggesting an age in the upper part of the above mentioned range. A strange fact is the apparent lack of K-type stars and the rather low X-ray luminosities of the few detected stars. The X-ray luminosities of NGC 2451 B show a much smaller scatter. Although this may be related to incompleteness resulting from the higher detection limit, the general distribution is more comparable to α Per. This is consistent with the slightly younger age suggested by the isochrone fits.

The time basis of 1 and 3 years between the individual ROSAT pointings allows a detailed study of X-ray variability. Consistent with previous studies, we have found a large number of stars to show slight but significant variations in their X-ray flux, yet there are only a few stars that varied by more than a factor 3. This again supports the idea that large X-ray variations due to activity cycles do not occur in young and active stars. In addition, we have found four X-ray flares that occured during the first PSPC pointing.

Substantial progress on membership of the individual stars attributed to one of the two clusters could be achieved by spectroscopic observations. We have therefore carried out a program on high-resolution spectroscopy in order to obtain radial and rotational velocities as well as lithium abundances. The results will be published in a forthcoming paper.

Acknowledgements. This work has been supported by the Deutsches Zentrum für Luft- und Raumfahrt (DLR) under grant 50 OR 9617 and by the Deutsche Forschungsgemeinschaft (DFG) under grants HU 546/4-1 and HU 546/6-1. We are indebted to K.-P. Schröder for providing us with the Pols et al. isochrones. This research has made use of the SIMBAD database, operated at CDS, Strasbourg, France.

References

Barbera, M., Micela, G., Collura, A., Murray, S. S., & Zombeck, M. V. 2000, ApJ, 545, 449
Barrado y Navascués, D., & Stauffer, J. R. 1998, ApJ, 506, 347
Baumgardt, H. 1998, A&A, 340, 402
Carrier, F., Burki, G., & Richard, G. 1999, A&A, 341, 469
Claria, J. J. 1985, A&AS, 59, 195
Eggen, O. J. 1983, AJ, 88, 197
Eggen, O. J. 1986, AJ, 92, 1074
Feinstein, A. 1966, PASP, 78, 301
Gagné, M., Caillault, J.-P., & Stauffer, J. R. 1995, ApJ, 450, 217
Girardi, L., Bertelli, G., Bressan, A., et al. 2002, A&A, 391, 195
Green, E. M., Demarque, P., & King, C. R. 1987, The Revised Yale Isochrones and Luminosity Functions, Yale Univ. Obs., New Haven
Groote, D., & Reimers, D. 1983, A&A, 119, 319
Harmer, S., Jeffries, R. D., Totten, E. J., & Pye, J. P. 2001, MNRAS, 324, 473
Hünsch, M. 2000, PASPC, 198, 455
Hünsch, M., & Reimers, D. 1993, A&A, 276, 161
Hünsch, M., & Reimers, D. 1995, A&A, 296, 509
Hünsch, M., & Schröder, K.-P. 1996, A&A, 309, L51
Hünsch, M., & Weidner, C. 2002, PASPC, in press
Hünsch, M., Schmitt, J. H. M. M., & Voges, W. 1998, A&AS, 132, 155
Hünsch, M., Randich, S., Hempel, M., Weidner, C., & Schmitt, J. H. M. M. 2003, A&A, in preparation
Jeffries, R. D., Thurston, M. R., & Pye, J. P. 1997, MNRAS, 287, 350
Johnson, H. L. 1966, ARA&A, 4, 193
Lejeune, T., Cuisinier, F., & Buser, R. 1997, A&AS, 125, 229
Lyngå, G., & Wramdemark, S. 1984, A&A, 132, 58
Maitzen, H. M., & Catalano, F. A. 1986, A&AS, 66, 37
Micela, G., Sciortino, S., Kashyap, V., et al. 1996, ApJS, 102, 75
Micela, G., Sciortino, S., Favata, F., Pallavicini, R., & Pye, J. 1999, A&A, 344, 83
Micela, G., Sciortino, S., Jeffries, R. D., Thurston, M. R., & Favata, F. 2000, A&A, 357, 909
Pastoriza, M. G., & Röpke, U. O. 1983, AJ, 88, 1769
Platais, I., Koszhurina-Platais, V., Barnes, S., & Horch, E. P. 1996, BAAS, 28, 822
Platais, I., Kozhurina-Platais, V., Barnes, S., et al. 2001, ApJ, 122, 1486
Pols, O. R., Schröder, K.-P., Hurley, J. R., Tout, C. A., & Eggleton, P. P. 1998, MNRAS, 298, 525
Prosser, C. F., Stauffer, J. R., Caillault, J.-P., et al. 1995, AJ, 110, 1229
Prosser, C. F., Randich, S., Stauffer, J. R., Schmitt, J. H. M. M., & Simon, T. 1996, AJ, 112, 1570
Randich, S. 1997, Mem. Soc. Astron. Ital., 68, 971
Randich, S., & Schmitt, J. H. M. M. 1995a, A&A, 298, 115
Randich, S., Schmitt, J. H. M. M., Prosser, C. F., & Stauffer, J. R. 1995b, A&A, 300, 134
Randich, S., Schmitt, J. H. M. M., Prosser, C. F., & Stauffer, J. R. 1996a, A&A, 305, 785
Randich, S., Schmitt, J. H. M. M., & Prosser, C. 1996b, A&A, 313, 827
Randich, S., Singh, K. P., Simon, T., Drake, S. A., & Schmitt, J. H. M. M. 1998, A&A, 337, 372
Reimers, D., Hünsch, M., Schmitt, J. H. M. M., & Toussaint, F. 1996, A&A, 310, 813
Robichon, N., Arenou, F., Mermilliod, J.-C., & Turon, C. 1999, A&A, 345, 471
Röser, S., & Bastian, U. 1994, A&A, 285, 875
Schmitt, J. H. M. M., Kahabka, P., Stauffer, J., & Piters, A. J. M. 1993, A&A, 277, 114
Schmitt, J. H. M. M. 1994, ApJS, 90, 735
Stauffer, J. R., Caillault, J.-P., Gagné, M., Prosser, C. F., & Hartmann, W. 1994, ApJS, 91, 625
Stern, R. A., Schmitt, J. H. M. M., & Kahabka, P. T. 1995, ApJ, 448, 683
Stetson, P. B. 1987, PASP, 99, 191
Sukyoung, Y., Demarque, P., Yong-Cheol, K., et al. 2001, ApJS, 136, 417
Terndrup, D. M., Pinsonneault, M., Jeffries, R. D., et al. 2002, ApJ, 576, 950
van den Oord, G. H. J., & Mewe, R. 1989, A&A, 213, 245
Weidner, C. 2000, Diploma Thesis, Univ. of Kiel, Kiel
Williams, P. M. 1966, Mon. Notes Astron. Soc. S. Afr., 25, 122
Williams, P. M. 1967a, Mon. Notes Astron. Soc. S. Afr., 26, 30
Williams, P. M. 1967b, Mon. Notes Astron. Soc. S. Afr., 26, 139
Zombeck, M. V., Barbera, M., Collura, A., & Murray, S. S. 1997, ApJ, 487, 69